

Evaluation of Iron Aluminide-Fly Ash Nanocomposite Prepared by Attritor Milling and Equal Channel Angular Extrusion Consolidation

Malur Srinivasan*, and Dipak Chavda**

An experimental investigation was conducted to evaluate the crystallite size and microhardness of mixtures iron aluminide (Fe_3Al) powder and Class C fly ash in different volume percentages, subjected to attritor milling and consolidation using Equal Channel Angular Extrusion (ECAE) process. Design of experiments was employed to select the lowest size of fly ash to be mixed with pre-milled iron aluminide powder. The results indicate that crystallite sizes in the low nano-range are obtained in all iron aluminide-fly ash compacts, qualifying the compact as a nanocomposite. The microhardness of the nanocomposite is lower than that of the nano-iron aluminide indicating the possibility of porosity being developed in fly ash during processing.

Keywords Iron aluminide, fly ash, Nanocomposite, Attritor milling, Pure shear consolidation, microhardness

1.0 INTRODUCTION

The main objective of this research was to prepare iron aluminide - fly ash nanocomposite using powder materials and to make preliminary studies on its behavior. In what follows the main constituents involved will be briefly described first and then the details of the research work will be provided.

1.1 Iron aluminide (Fe_3Al).

This is an intermetallic compound of iron and aluminum and has excellent oxidation and sulfidation resistance at intermediate temperatures. In Figure 1 is shown the phase diagram of iron-aluminum alloy

As seen in the phase diagram, Fe_3Al can occur in any of the three different kinds of crystal structure depending on the temperature: an ordered D0₃-type superlattice structure below about 550°C, an

ordered B2-type superlattice between about 550° and 750°C (1022° and 1382°F), and disordered BCC at higher temperatures.

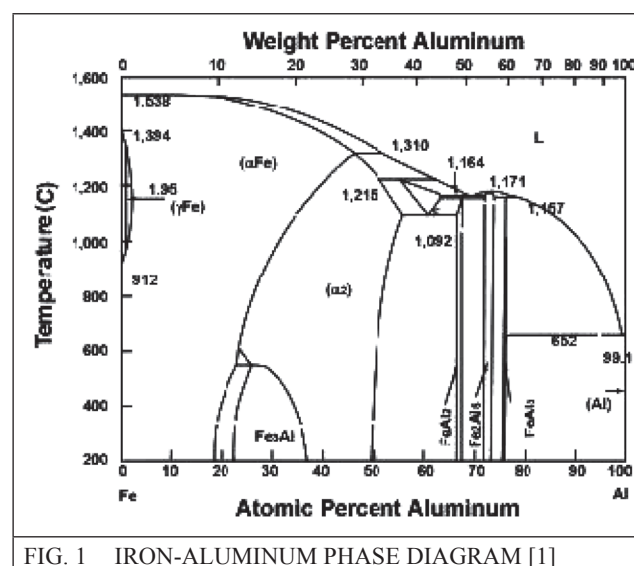


FIG. 1 IRON-ALUMINUM PHASE DIAGRAM [1]

The B2-type structure is basically BCC, while D0₃ is comprised of eight BCC cells stacked two deep in each direction and results in the

* Department of Mechanical Engineering Lamar University Beaumont, Texas 77710, USA. Email : malursrinivasan@lamar.edu

** Engineering Project Manager, SBM, Offshore USA.

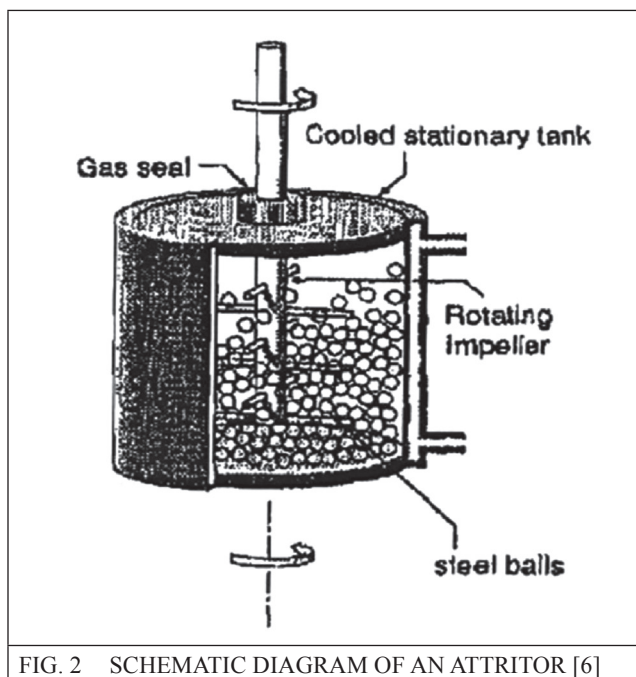
same symmetry as an FCC structure [1]. Room temperature ductility of Fe_3Al is sensitive to environmental conditions, particularly to moisture [2-3].

1.2 Fly ash

Fly ash is a finely divided coal combustion byproduct (CCB) collected by electrostatic precipitators from flue gases. The particles are generally less than 250 micrometers in size, have hollow spheroidal shape (similar to cenospheres), variable density in the range of 3-0.6, melting point above 1000°C , low thermal conductivity and are mostly chemically inert [4]. The American Society for Testing and Materials (ASTM) has identified two classes of fly ash, Class F from bituminous coal and Class C from subbituminous and lignite coal [5]. In the present investigation, Class C fly ash was used. This has typically 25-42% SiO_2 , 15-21% Al_2O_3 , 5-10% Fe_2O_3 , 17-32% CaO , 4-12.5% MgO , as the major constituents.

1.3 Attritor Milling

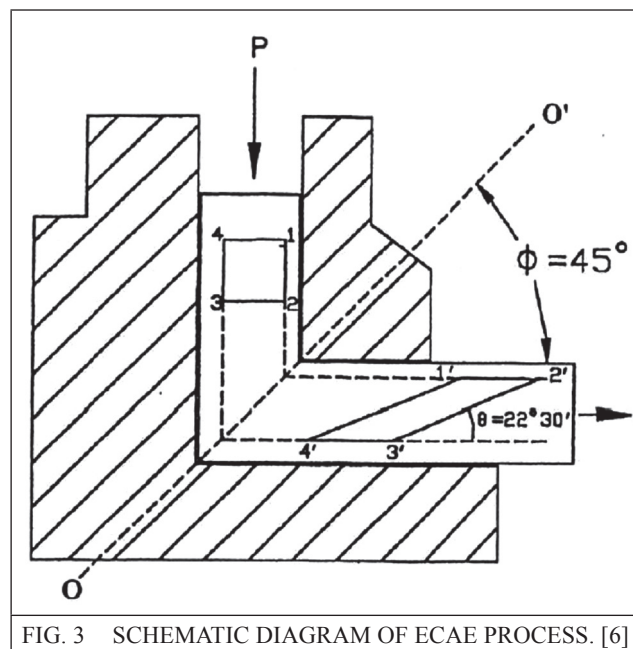
In Figure 2 is shown a schematic view of an attritor. It is a vertically oriented ball mill with an internal shaft with arms that can agitate the charge (powders and grinding balls).



A water-cooled jacket helps to control the temperature of the process. The milling is performed in a protective atmosphere; argon was used in our experiments. Under proper conditions, nanostructured powder can be obtained after milling. After milling, the attritor chamber is disconnected and the milled material with the balls is emptied into containers in a glove box with protective atmosphere. The filling of the chamber is also done inside the glove box to prevent contamination with ambient air and moisture.

1.4 Equal Channel Angular Extrusion (ECAE) Process.

In Figure 3 is shown a schematic view of the ECAE process. The basis of this process is the application of repeated simple shear to a billet in which the milled powder is housed in drilled holes. The intense and uniform plastic deformation caused by pure shear in this process is capable of producing not only compaction of the powder but further refining the structure of the powder.



The figure shows a 0.025 m square stainless steel bar subjected to ECAE. The milled powder was placed in four symmetric holes of 0.003 m diameter drilled in the bar. The holes were then sealed at the top by using ion beam welding at Ames DOE Laboratory at Ames, Iowa. After

annealing the sealed billet at 12000C for 1 hr in argon, it was extruded using the ECAE facility at Texas A&M University. Route A, in which the same orientation is maintained between the shear plane and the shear direction with respect to the extrusion direction was used. This route is meant to better compaction as discussed by Parasiris [7]. The four billets of consolidated material were then extracted from each stainless bar and annealed again in argon for 1 hr at 14000C for testing and analysis.

1.5 Nanostructured Materials

The novelty of nanostructured materials is that they have a significant fraction of the total atoms being present at the grain boundaries unlike their micro-grained counterparts [6-20 Chavda]. The grain size of nanostructured materials is in the range of less than 1000 nm to a few nm. If the grain size is more than about 10 nm, Hall-Petch relationship is observed, the yield stress increasing with decreasing grain size, as in micro-grained materials. However, if the grain size is below about 10 nm, inverse Hall-Petch relationship is observed, the yield stress decreasing with decreasing grain size [8]. Nanostructured materials can be exceptionally strong, hard and ductile at high temperatures. They can also be wear resistant, erosion resistant and corrosion resistant. They are also more hot-formable than their conventional micro-grained counterparts.

2.0 EXPERIMENTAL PROCEDURE [9].

2.1 The following steps were followed in the present investigation.

2.1.1 Selection of attritor milling parameters using 2³ factorial design of experiments for minimum crystallite size of fly ash.

For this purpose, three attritor milling parameters were considered: milling speed, milling time and powder-to-ball ratio. The upper values were 550 rpm, 40 hr and 30:1, respectively for the three parameters. The corresponding lower values were 150 rpm, 10 hr and 10:1, respectively. Eight

combinations of these parameters were used for milling of fly ash as shown in Table 1, using the equipment shown in Figure 1.

2.1.2 Preparation of Fe₃Al powder in the attritor.

For this purpose, commercial purity iron (99.9% pure) and commercial purity aluminum (99.9% pure) were mixed in proportion of 86.13 wt.% iron and 13.87 wt.% aluminum and milled for 100 hr at a speed of 150 rpm and ball-to-powder ratio to produce Fe₃Al powder.

2.1.3. X-ray diffraction of the powders after steps 2.1.1 and 2.1.2.

For this purpose, a collection of random samples of the milled fly ash powder was mounted in an air-setting amorphous polymer block and subjected to powder diffraction using an X-ray diffractometer. Scherrer's [10] formula gives the relationship between crystallite size of the powder, pure diffraction breadth at half maximum intensity and Bragg angle. The pure diffraction breadth at half intensity is obtained after applying correction factors to the observed diffraction breadth at half intensity as detailed by Bertram [11]. For copper K α radiation, the final equation obtained is

$$D = \frac{79.51}{\beta \cos \theta} \quad \dots(1)$$

where, D = crystallite size, β is pure diffraction breadth at half maximum intensity determined after correcting the observed diffraction peak breadth at half maximum intensity in radians, and θ is half-Bragg angle in radians.

2.1.4. Attritor milling of a mixture of four different volume percentages of fly ash with Fe₃Al using attritor milling parameters based on step 2.1.1.

For this purpose, Fe₃Al powder was mixed successively with 10 vol.%, 15 vol.%, 20 vol.% and 25 vol.% of fly ash for attritor milling with parameters selected based on step 2.1.1.

2.1.5 ECAE consolidation of powders in step 2.1.3.

This was performed at the facility available at Texas A&M University at College Station, Texas, after filling four holes drilled into the top of a stainless steel bar to be extruded by ECAE and getting the top of the holes sealed by ion beam welding at Ames Research Laboratory in Iowa, using the Route A pass shown schematically in Figure 2.

2.1.6 Annealing of ECAE bar at 14000C for 1 hr in argon atmosphere.

2.1.7 Determination of the microhardness of the consolidated samples extracted from

ECAE bar using a Vickers hardness tester at Lamar University, Beaumont, Texas.

2.1.8 Determination of the crystallite size of Fe₃Al-fly ash compacts.

For this purpose, the compacts were ground and subjected to X-ray diffraction in a manner similar to the one described in section 2.1.3 to determine the crystallite size after ECAE.

3.0 RESULTS AND DISCUSSION.

In Table 1 are shown the combination of different attritor milling parameters in each of the eight (2³) factorial design experiments and the average crystallite size of fly ash.

TABLE 1				
CRYSTALLITE SIZE OF FLY ASH FOR DIFFERENT COMBINATION OF ATTRITOR MILLING PARAMETERS				
Experiment Number	Ball-to-powder weight ratio A	Milling speed Rpm B	Milling time Hr C	Average crystallite size nm
1	10:1	150	10	25
2	10:1	150	40	51
3	10:1	500	40	81
4	10:1	500	10	52
5	30:1	150	10	153
6	30:1	500	10	50
7	30:1	150	40	67
8	30:1	500	40	55

The regression equation developed using these results [12] is:

$$C.S. = 66.7 + 14.6 A - 7.2 B - 3.3 C - 21.6 AB + 11.9 BC - 17.0 AC + 11.0 ABC \dots(2)$$

where, C.S. is crystallite size in nm, the coefficient of A is the effect of ball-to-powder weight ratio, the coefficient of B is the effect of milling speed, the coefficient of C is the effect of milling time, the coefficient of AB is the effect of interaction of ball-to-powder weight ratio and the milling speed, the coefficient of AC is the effect of interaction

of ball-to-powder ratio and milling time, the coefficient of BC is the effect of interaction of milling speed and milling time, the coefficient off ABC is the effect of interaction of all the three parameters.

Considering the object as obtaining the lowest crystallite size, the combination of milling parameters in experiment 1 (lower ball-to-powder ratio, lower milling speed and lower milling time) gives the lowest crystallite size (best result) and the combination of milling parameters in experiment 5 (higher ball-to-powder ratio, lower milling speed and lower milling time) gives the

highest crystallite size (worst result). These may also be deduced from equation (1) by taking (+1) for higher values and (-1) for lower values of the parameters A, B and C.

Based on these observations it was decided to attritor mill a mixture of Fe₃Al powder prepared as described in section 2.1.2 and as-received fly ash in weight percentages stated in section 2.1.4, using the milling parameters: 10:1 ball-to-powder ratio by weight milling speed of 150 rpm and milling time of 10 hr. The milled powders were emptied from the attritor chamber in a glove box with argon atmosphere, carefully separated from the stainless steel ball and carefully stored in water-tight and air-tight containers. The powders were then subjected to ECAE consolidation as described in section 2.1.5. After ECAE consolidation, the extrudates were annealed as per section 2.1.6 and the microhardness of the extracted Fe₃Al-fly ash compacts were determined as per section 2.1.7. The crystallite sizes of the compacts were then determined as per section 2.1.8. In Table 2 are shown the microhardness values of the compacts along with their crystallite sizes. It is seen that compacts both Fe₃Al without fly ash and Fe₃Al with different volume percentages of fly ash have crystallite sizes in the low nanometer range and therefore Fe₃Al-fly ash compacts prepared in this work can be classified as Nano composites.

Vol.% Fly Ash in Fe ₃ Al	Microhardness VHN	Crystallite size nm
0	521	29
10	386	47
15	382	86
20	382	51
25	374	52

In Figure 2 is shown a plot of microhardness vs. volume percent of fly ash in Fe₃Al, drawn from the data in Table 2.

It is seen in Table 2 and Figure 2 that the microhardness of Fe₃Al-Fly ash nano-composite lies in a narrow range of 374 VHN to 386

VHN, as compared to the microhardness of 521 VHN for nanostructured Fe₃Al without fly ash. Thus there is an average drop of about 27% in microhardness, when fly ash is added in different volume percentages to Fe₃Al.

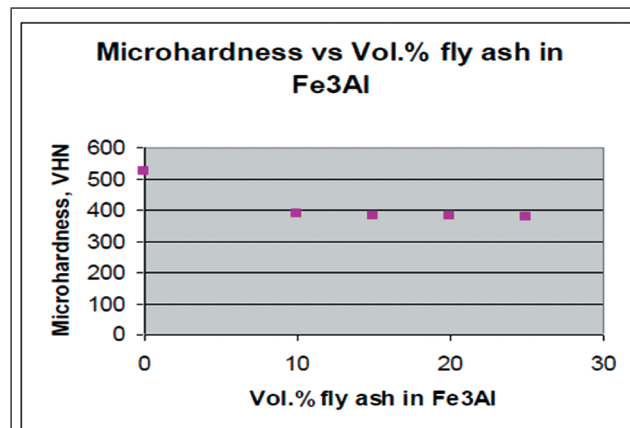


FIG. 2 MICROHARDNESS VS. VOLUME PERCENT OF FLY ASH IN FE₃AL

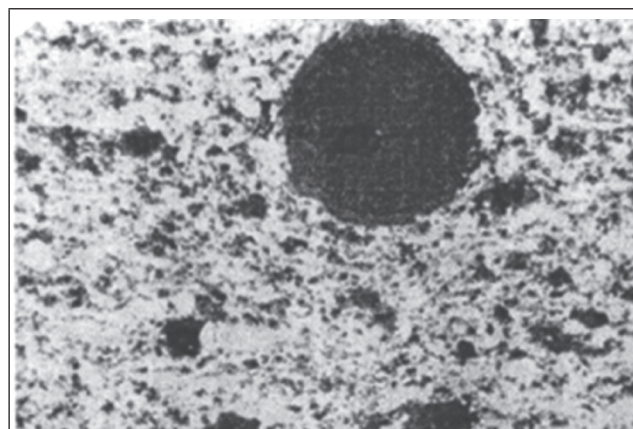


FIG. 3 OPTICAL PHOTOMICROGRAPH OF Fe₃Al-25VOL.% FLY ASH (X1000)

To throw light on the reason for the drop in microhardness when fly ash is added to Fe₃Al, microstructure of the compacts was examined. A selected photomicrograph showing an isolated fly ash particle in the mid-top region is shown in Figure 3. It is seen that the fly ash particle is porous, but the resolution is limited as it is an optical photomicrograph. Study of literature revealed that when observed in a scanning electron microscope, fly ash particle can have interconnected porosity throughout, when heated to temperatures above 10000C. A typical SEM photograph illustrating this point is shown in Figure 4 [13]. This seems to be the major reason why the microhardness of the nanocomposite drops in the present study, as the ECAE extrudates

(and consequently, the compacts) were annealed at 14000C. Interestingly, the tensile strength and percent elongation both decreased with respect to Fe₃Al without fly ash, when lightly attritor milled mixtures of Fe₃Al and fly ash were conventionally extruded at 12000C and hot forged before tensile testing [14], indicating that porosity development in fly ash as a result of high temperature extrusion may have been responsible for these results as well.

It is thus clear that porosity cannot be avoided in Fe₃Al-Fly ash nanocomposites prepared by attritor milling and ECAE consolidation, as the stainless billets with the sintered powders inside are annealed at 14000C. A similar situation seems to be present in conventionally extruded (at 12000C) lightly milled Fe₃Al-Fly ash mixtures as well. Thus it is unlikely that fly ash will have any strengthening effect on Fe₃Al when the composite is produced by exposure to temperatures above 11500C.

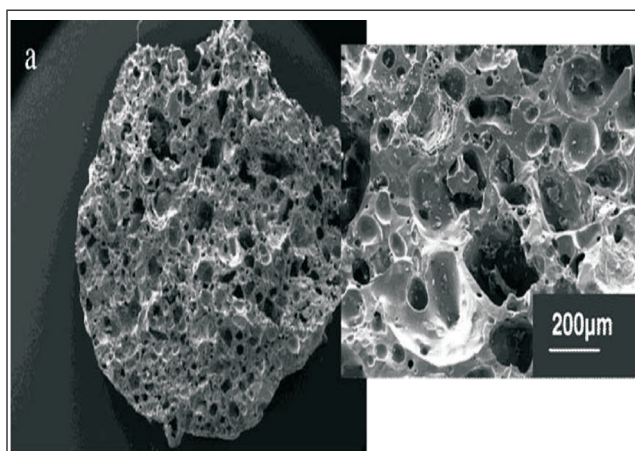


FIG. 4 POROSITY DEVELOPMENT IN FLY ASH BY THERMAL HEATING AT 1150°C [13]
[HTTP://DIGITAL.CSIC.ES/BITSTREAM/10261/6338/1/1.PDF](http://digital.csic.es/bitstream/10261/6338/1/1.PDF)

It has been stated [15] that Fe₃Al filters with pores introduced by controlled sintering are useful in separating solid particles from flue gases in coal-fired thermal plants. The results of this paper suggest that by adding fly ash to Fe₃Al there will be built-in porosity without the need for controlled sintering. It is pertinent to state in this context that if strengthening of Fe₃Al is required, yttria addition will be helpful [16].

4.0 CONCLUSIONS

- 4.1 Factorial design of experiments is useful in determining the extent of significance of the ball-to-powder ratio, milling speed and milling time and their interactions on the crystallite size of attritor milled fly ash.
- 4.2 The crystallite sizes attritor milled and ECAE consolidated Fe₃Al as well as Fe₃Al-Fly ash composites in the present work all have crystallite sizes in the low nano-range indicating that the process adopted in this research is suitable for producing both nanostructured Fe₃Al and Fe₃Al-fly ash nanocomposites.
- 4.3 The microhardness of Fe₃Al-fly ash nanocomposite decreases by about 27% compared to that of nanostructured Fe₃Al under the experimental conditions investigated.

REFERENCES

- [1] S A David, JA Horton, CGMcKamey, T Zacharia and RW Reed, "Welding Journal Supplement", September p373,1989, http://www.aws.org/wj/supplement/WJ_1989_09_s372.pdf.
- [2] C T Liu, C G McKamey and EH Lee, Scripta Metallurgica, Vol.23, p875,1989.
- [3] C T Liu, C G McKamey and EH Lee, Scripta Metallurgica, Vol.24, p385,1990.
- [4] R Majko, "Coal Combustion Byproducts", Fly Ash Resource Center, <http://www.geocities.com/CapeCanevaral/Launchpad/2095/flyash.html>.
- [5] R Majko, Materials Research, Fly Ash Resource Center, <http://www.geocities.com/CapeCanevaral/Launchpad/2095/flyash.html>.
- [6] K Ramakrishnan, Doctor of Engineering dissertation, Lamar University, Beaumont, Texas, 2001.
- [7] A Parasiris, MS thesis, Texas A&M University, College Station, Texas, 1999.

- [8] C E Carlton and PJ Ferreira, *ActaMaterialia*, Vol.55, p3749-3755,2007.
- [9] D Chavda, Master of Engineering Science thesis, Lamar University, Beaumont, Texas, 2001.
- [10] P Scherrer, *Gottingen Nachr*, New York, John Wiley, p98, 1918.
- [11] S F Bartram in “Handbook of X-rays for Diffraction, Emission, Absorption and Microscopy”, New York, Emmett F. Kaelble, pp17.1-17.6,1967.
- [12] D C Montgomery, “Design and Analysis of Experiments”, 3rd ed, New York, John Wiley, p270, 1991.
- [13] M Aineto, A Acosta, J M Rincon and M Romero, <http://digital.csic.es/bitstream/10261/6338/1/1.pdf>.
- [14] M N Srinivasan, Unpublished work done at Oak Ridge National Laboratory, Tennessee, 1994.
- [15] V K Sikka in *Processing, Properties and Applications of Iron Aluminides*, J. H. Schneibel and M. A. Crimp. Editors, Proceedings of Symposium, Annual Meeting of Minerals, Metals and Materials Society, San Francisco, California, p8, 1994.
- [16] M N Srinivasan and V K Sikka in *Processing, Properties and Applications of Iron Aluminides*, J H Schneibel and M A Crimp. Editors, Proceedings of Symposium on Iron Aluminides, Annual Meeting of Minerals, Metals and Materials Society, San Francisco, California, p69-77,1994.

